Simulation of primary recrystallization from TEM observations and neutron diffraction measurements

T Baudin, D Solas, A. L. L Etter, D Ceccaldi, R Penelle

SIMULATION OF PRIMARY RECRYSTALLIZATION FROM TEM OBSERVATIONS AND NEUTRON DIFFRACTION MEASUREMENTS

T. Baudin, D. Solas, A.L. Etter, D. Ceccaldi and R. Penelle

Université de Paris Sud, ICMMO
Laboratoire de physico-chimie de l'état solide, UMR CNRS 8648,
Bâtiment 410, 91405 Orsay Cedex, France.

Keywords : Computer simulation, Primary recrystallization, Stored energy, TEM

Abstract: The Monte Carlo method is used to simulate primary recrystallization in a fcc nickel iron sheet deformed by cold rolling. Experimental data, such as the microstructure, the microtexture characterized by TEM and the stored energy estimated by neutron diffraction, constitute the input values for the calculation. This approach allows to reproduce experimental observations i.e. the bulging of cube cells during annealing.

Introduction

A simulation procedure of grain growth has been recently implemented using an experimental microstructure measured by Orientation Imaging Microscopy (OIM^{TM}) (1) as an input data set (2). Several studies (3, 4, 5, 6) have then proved the interest in this type of Monte Carlo simulation-experiment coupling.

Then, Engler (3) has extended this approach to primary recrystallization simulation, using the quality of EBSD (Electron Back Scattered Diffraction) patterns to estimate the stored energy, which is the main driving force for recrystallization. The EBSD spatial resolution is about 0.5 μm with a classical W filament-SEM. It can be improved with a FEGSEM but if the dislocation density is too high or if the size of the dislocation cells is very small, the EBSD patterns are blurred and so cannot be correctly indexed. As a consequence, in some cases the as-deformed microstructure cannot be completely described by OIM and therefore some regions remain undefined. This difficulty can be bypassed using transmission electron microscopy (TEM).

So a new model based on data derived from TEM texture analysis has been developed (7). The described approach is unfortunately limited because of the lack of stored energy values. These values can however be estimated by X-ray or neutron diffraction. So, Rajmohan and Szpunar (8) have simulated primary recrystallization of aluminium alloys from theoretical initial microstructure, using experimental stored energy values measured by X-ray diffraction.

Then, a logical way to improve the simulation consists in performing calculations from a microstructure characterized by TEM using orientation-dependant stored energy estimated by neutron diffraction measurements (9). This is the purpose of the present paper in

the case of a FeNi alloy. Such a coupling between results defined at a microscopic scale (microstructure characterized by TEM) and at a macroscopic scale (stored energy calculated from neutron diffraction measurements) has never been proposed in the literature at our knowledge.

Material and experimental procedure

In most of their applications, Fe-Ni alloys are used in the form of thin strip. In particular, this is true for shadow masks placed immediately behind the screen in color television tubes to focus the electron beam on the phosphors of the right color. The thin strip is obtained by cold rolling, involving severe reductions. Then, a heat treatment leads to a sharp cube ({001}<100>) texture by primary recrystallization (10, 11).

In order to obtain the largest amount of information about the microstructure, the samples were prepared from the ND-TD plane of a cold rolled (95% reduction) Fe-36%Ni sheet (12). Figure 1 shows a microstructure in which a cube band is formed of well-recovered cells. Each part of the microstructure has been defined from a crystallographic point of view from Kikuchi and spot diffraction patterns (13).

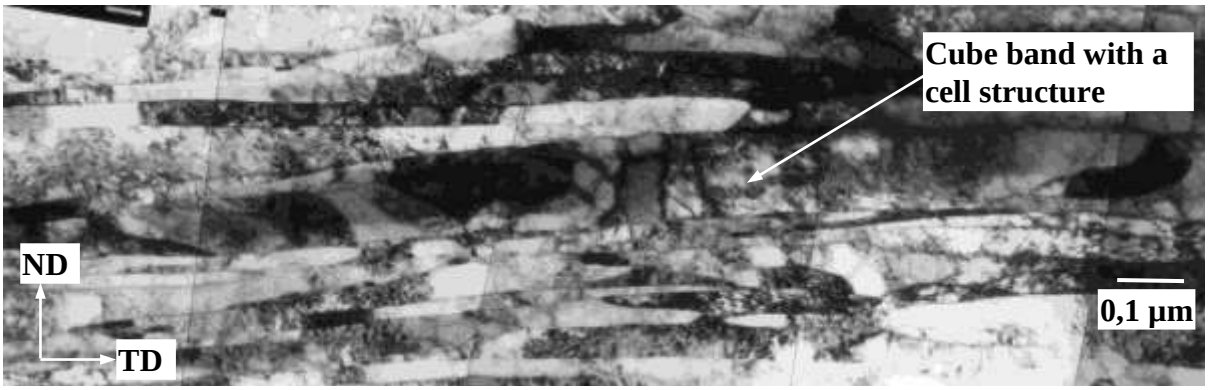

Figure 1. Microstructure observed by TEM in a 95% cold rolled sheet (12).

Taking into account experimental observations after short time annealing, the most likely recrystallization mechanism can be described as follows (14): the critical size of cube cells is supposed to be reached by either cell coalescence or growth into the orientation gradient observed in the cube bands (15). However, this recovery period is short and so, the critical size is quickly reached. Then, the cells can grow into the matrix because of the large stored energy difference and the presence of high angle grain boundaries. The stored energy has been estimated for each orientation in the Euler space from neutron diffraction measurements (9, 16). For 95% cold rolling, the cube orientation stored energy is about 10 J/mol, whereas the stored energy of the main texture components (B {110}<112>, S {123}<634> and C {112}<111>) is about twice. The low stored energy observed for the cube orientation gives the cube sub-grains an evident advantage to grow in the neighboring grains with highest energy. This explains the bulging of “cube grains”, evidenced by TEM observation (figure 2). Let us note that the figures 1 and 2 are micrographs of two different areas. Indeed, after annealing, TEM observations must be performed in the bulk of the specimen to avoid surface effects.

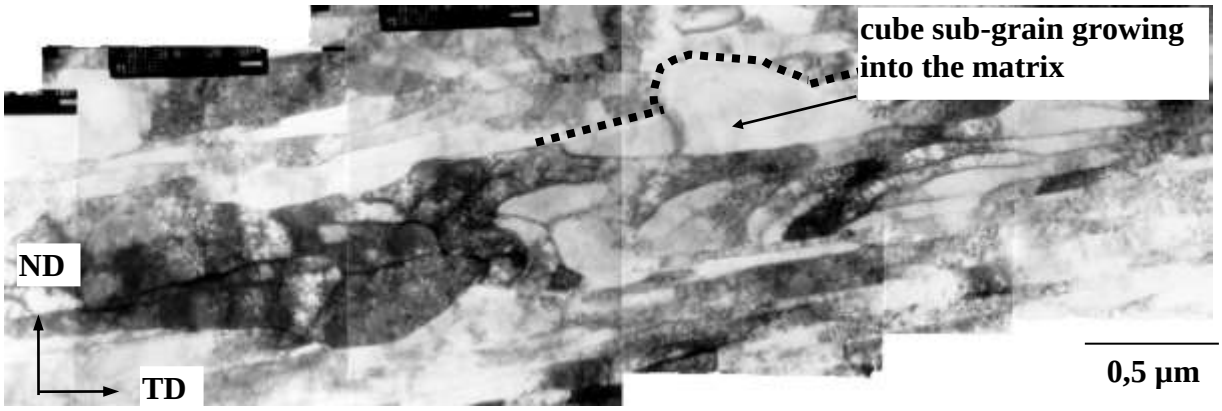

Figure 2. TEM micrograph showing a cube band in the 95% cold rolled and 2 min. annealed sample (14).

Numerical procedure

The model based on the Monte Carlo simulation has been described in a previous paper (7). The stored energy was then adjusted to reproduce the experimental observations. In the present study, the value of the driving force is not fitted but is measured by neutron diffraction performed on bulk samples (16). Then, it is possible to assign a stored energy value to each crystallographic orientation described in the Euler space. Figure 3 shows the stored energy plotted as a function of φ_1 and ϕ for constant φ_2 sections.

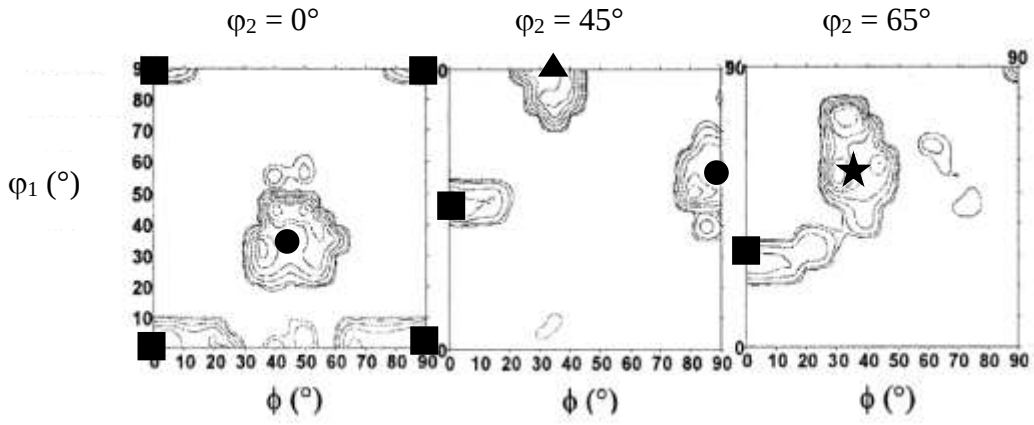

Figure 3. Stored energy distribution function of the 95% cold rolled specimen. Levels: 1, 2, 5, 9, 14, 18 and 26 J/mol. The ideal orientation positions are specified on constant φ_2 sections (0°, 45°, 65°): B - black circle, S - black star, C - black triangle and Cube - black square (16).

So, the TEM microstructure (figure 1) can be characterized by all the morphological, crystallographic and stored energy parameters as an ASCII file (980 x 234 points) used for the Monte Carlo simulation (17). Figures 4 and 5 describe the input data of the simulation. Figure 4 shows the crystallographic orientation distribution (sketched via misorientations from the cube orientation). Figure 5 shows the stored energy distribution through the microstructure.

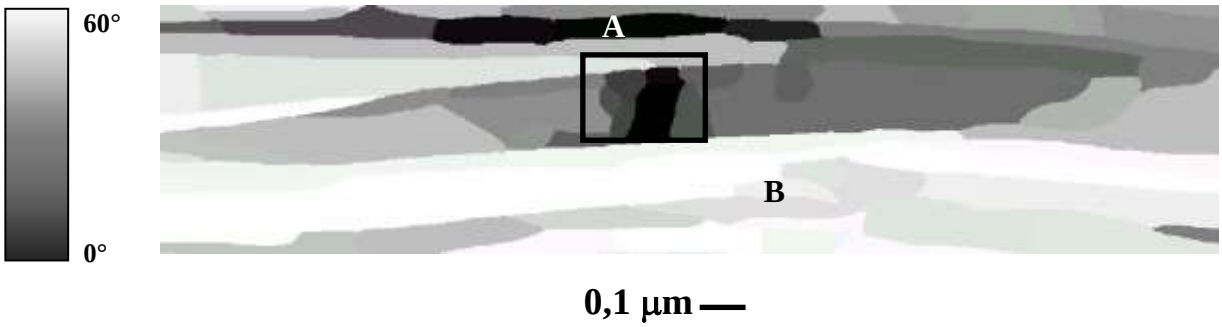

Figure 4. Initial microstructure used as input data for the simulation. The microstructure, shown in figure 1, is here presented using a grey level gradient defined as a function of the misorientation from the cube orientation that corresponds to the black level ($\Delta\theta = 0°$).

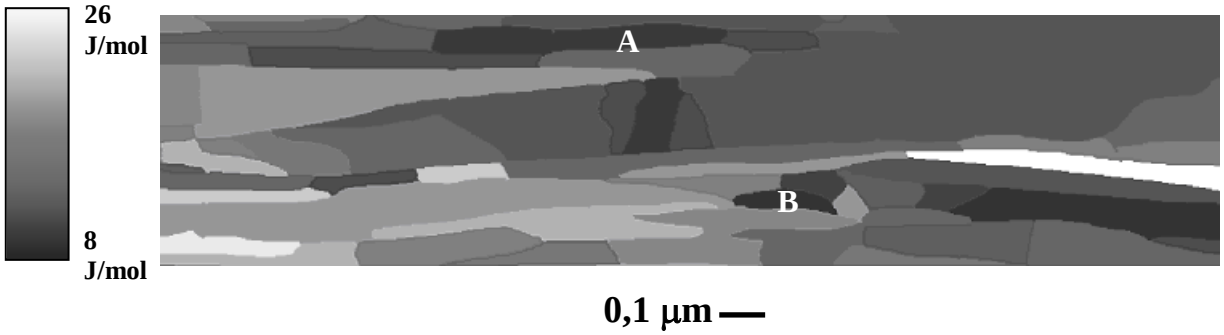

Figure 5. Initial microstructure used as input data of the simulation. The microstructure, shown in figure 1, is here presented using a grey level gradient defined as a function of the stored energy (black level = 8 J/mol and white level = 26 J/mol).

As described above, because the recovery time necessary for a successful nucleus to reach a critical size is very short in the present simulation, it is assumed that the cube cells can directly grow into the matrix. Figure 6 shows a zoom of the microstructure inside the black rectangle drawn in figure 4 after simulation. In the first steps of the recrystallization simulation, the bulging of a prior boundary leads to the growth of cube or near-cube cells into the matrix (cells C and D). This result is similar to the observed experimental phenomenon (figure 2), even if it does not correspond to the same observed area.

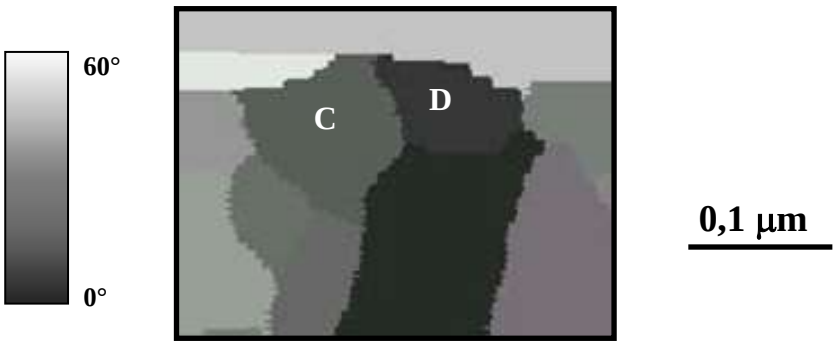

Figure 6. Simulated annealed microstructure. The microstructure is described using a grey level gradient defined as a function of the misorientation from the cube orientation that corresponds to the black level.

Because the stored energy difference and the misorientation between the nuclei and the matrix are important, cube sub-grains inside the black rectangle can develop. Other cube sub-grains (for example, sub-grain A, figures 4 and 5) do not grow, at least during the first steps of the simulation, because of a low stored energy difference with their neighbors (figure 5). On the contrary, this difference is large for sub-grain B that has not the cube orientation (figure 4) but it does not develop because of a low misorientation with its neighbors (figure 4).

Conclusion

Up to now, the primary recrystallization simulations based on theoretical or experimental microstructures were not very powerful since the stored energy had to be adjusted to reproduce the experimental observations of sub-grain growth (see (7)). So, no prediction was possible. In all those models, the lack of data was obvious.

In the present work, experimental multi-scale data, such as orientation-dependant stored energy assessed by neutron diffraction and crystallographic orientation measured by TEM, have been introduced in the simulation of the primary recrystallization of a Fe-36%Ni alloy. The experimental growth of cube or near cube sub-grains is quite well predicted by the simulation. These sub-grains can grow into the matrix because of their low stored energy, the large stored energy difference with their neighbors and the presence of prior high angle boundaries. Contrary to previous works, no stored energy adjustment has been necessary to reproduce the experimental growth observations.

These results are promising even if many improvements remain to be done. For example, the grain boundary energies used in the calculation are still adjusted and not experimental. Moreover, the neutron diffraction technique allows to affect an averaged stored energy to a given orientation but does not take into account the stored energy gradient inside a grain (near the boundaries and inside the grain) or a sub-grain. A solution could consist in using the simulated deformation stored energy (18). Such calculation based on the finite element method is actually performed from OIM measurements but unfortunately it is not ready to work from TEM measurements.

Acknowledgement

The authors would like to thank the Imphy-Ugine-Precision Company and particularly P.L. Reydet, P. Cremer and F. Duffaut, for providing the Fe-36%Ni alloy.

References

1. B.L. Adams, S.I. Wright and K. Kunze, Met. Trans. A, 24A, 819 (1993).
2. T. Baudin, P. Paillard and R. Penelle, Scripta Materialia, 36, 789 (1997).
3. O. Engler, Proc. of the 19th Riso Int. Symp. on Materials Science, Roskilde, Denmark, September 1998, ed. J.V. Carstensen et al., 253 (1998).
4. T. Baudin, P. Paillard and R. Penelle, Scripta Materialia, 40, 1111 (1999).
5. M. Kobayashi, Y. Takayama, H. Kato and T. Shibayanagi, Proc. of the First Joint Int. Conf., eds G. Gottstein and D.A. Molodov, Springer-Verlag, August 27-31, 233 (2001).
6. J. Tarasiuk, Ph. Gerber, B. Bacroix and K. Piekos, Proc. of the13th Int. Conf. on Textures of Materials, Seoul, Korea, August 26-30, 395 (2002).
7. T. Baudin, F. Julliard, P. Paillard and R. Penelle, Scripta Materialia, 43, 63 (2000).
8. N. Rajmohan and J.A. Szpunar, Acta mater., 48, 3327 (2000).
9. V. Branger, M.H. Mathon, T. Baudin and R. Penelle, Proc. of the 21st Riso Int. Symposium, 4-8 September 2000, Risoe National Laboratory, Roskilde, Denmark, eds. N. Hansen et al., 257 (2000).
10. A Hundred Years after the Discovery of Invar …, The iron-nickel alloys, ed. G. Béranger et al., Tec & Doc-Lavoisier (1996).
11. F. Julliard, Etude des mécanismes de recristallisation dans l'Invar, alliage Fe-36%Ni, Thèse, Univ. de Paris-Sud Orsay (2001).
12. F. Julliard, T. Baudin and R. Penelle, Archives of Metallurgy, 45, 33 (2000).
13. S. Zaefferer, J. Appl. Cryst., 33, 10 (2000).
14. R. Penelle, T. Baudin, A.L. Etter and D. Solas, Proc. of the13th Int. Conf. on Textures of Materials, Seoul, Korea, August 26-30, 739 (2002).
15. S. Zaefferer, T. Baudin and R. Penelle, Acta Materialia, 49, 1105 (2001).
16. A.L. Etter, M.H. Mathon, T. Baudin, V. Branger and R. Penelle, Scripta Materialia, 46, 311 (2002).
17. D. Solas, C.N. Tome, O. Engler and H.R. Wenk, Proc. of the 4th Int. Conf. on Recrystallization and Related Phenomena, Tsukuba, Japan, July 13-16, 639 (1999).
18. P. Erieau and C. Rey, Proc. of the13th Int. Conf. on Textures of Materials, Seoul, Korea, August 26-30, 389 (2002).